Journal of Insects as Food and Feed, 2022; 8 (2): 169-183

Wageningen Academic Publishers

Characterisation of black soldier fly larva protein before and after conjugation by the Maillard reaction

B. Zozo[1], M.M. Wicht[1*], V.V. Mshayisa[2] and J. van Wyk[2]

[1]Department of Chemistry, Cape Peninsula University of Technology, Bellville, 7535, South Africa; [2]Department of Food Science and Technology, Cape Peninsula University of Technology, Bellville, 7535, South Africa; wichtm@cput.ac.za

Received: 26 January 2021 / Accepted: 2 June 2021
© 2021 Wageningen Academic Publishers

OPEN ACCESS

RESEARCH ARTICLE

Abstract

Black soldier fly has been proposed as an alternative protein source sustainable for both food and feed due to its nutritional composition. The functional properties of this protein can be improved by inducing the Maillard reaction (MR) in protein-sugar mixtures. This study focused on the conjugation and characterisation of black soldier fly larvae (BSFL) proteins and conjugates. The defatted BSFL larvae were subjected to protein extraction at an alkaline pH. The protein extract was then conjugated with glucose. The BSFL protein and glucose were mixed at (2:1 w/w, pH 9), incubated at 50, 70, and 90 °C for 30, 60, 90 and 120 min. The products obtained were then characterised and compared. The changes were confirmed by universal attenuated total reflectance Fourier-transform infrared spectroscopy (UATR-FTIR), scanning electron microscopy, thermal gravimetric analysis and differential scanning calorimetry. UATR-FTIR combined with principal component analysis monitored the protein-sugar conjugates, to show the structural difference among heated proteins and conjugates. The heating treatments resulted in the unfolding and reduction of the protein molecule aggregation. The protein extract from the larvae was rich in protein content (67±0.78%) and displayed good essential amino acids (EAA) in sufficient quantities to meet the dietary requirements for humans. The EAA quantities of the conjugates decreased due to the MR treatment. The conjugates showed a significant decrease in the lysine content as a function of reaction temperature and time at 90 °C and 120 min, respectively. FTIR indicated that the amide I and II bands of the protein were altered by the MR. The increased T_{max} (the temperature at which decomposition is completed) demonstrated that the conjugation of the protein with glucose improved the thermal stability, remarkably. These results suggested that MR with glucose can be a promising way to improve the thermal properties of BSFL protein.

Keywords: insect protein, black soldier fly, Maillard reaction, structural analysis, nutrition

1. Introduction

The rapid world population growth is severely restricting conventional food sources (Wang *et al.*, 2017) and growing protein demand cannot be met by the current livestock, poultry and plant protein production system. For this reason, insects are proposed as an alternative source for food and feed because of their nutritional composition and their sustainable production when compared to known protein sources (Janssen *et al.*, 2017; Osimani *et al.*, 2017; Purschke *et al.*, 2018). Black soldier fly (BSF) is one of the insects engendering interest globally as a sustainable protein source (Müller *et al.*, 2017) due to its high protein content for chicken (Schiavone *et al.*, 2017), fish (Belforti *et al.*, 2015; Henry *et al.*, 2015; Renna *et al.*, 2017) and swine feed (Makkar *et al.*, 2014). Additionally, it has been exploited for biodiesel production because of its high-fat content (Feng *et al.*, 2018; Wang *et al.*, 2017). Despite human perception against insects as food, consumers are willing to include insects in their dishes in an unrecognised form, such as a modified product, powders and pastes (Balzan *et al.*, 2016; Schösler *et al.*, 2012). Therefore, the potential for BSF larvae protein to be exploited for human consumption is a prospect, although requiring additional protein scientific information.

The unavailable information on the extent to stabilise insect protein via Maillard reaction is of interest. Proteins are important food ingredients because they have the ability to change the taste, texture and appearance of the foods. However, proteins are very unstable in certain conditions of temperature, pH or the presence of organic solvents. In a study conducted by Bußler *et al.* (2016) the solubility of the proteins was found to be dependent on the pH during the extraction process. Other extraction conditions (pH, ionic strength and temperature) were altered and the effect on the composition and properties of recovered insect flour fraction were investigated. Thus, researchers have enhanced protein stability under these unfavourable conditions by interacting with saccharides (Akhtar and Ding, 2017; Dickinson, 2015; Evans *et al.,* 2013). Saccharides are high molecular weight polymers with very high stability (De Oliveira *et al.*, 2016). Therefore, by combining the properties of these two compounds through conjugations, it is possible to obtain a product with higher stability (Akhtar *et al.*, 2017; Dickinson, 2015; Evans *et al.*, 2013).

Conjugates are best obtained using the Maillard reaction (MR) (De Oliveira *et al.*, 2016; Liu *et al.*, 2016) for the ideal and safest method in protein modification (Feng *et al.*, 2018; Ifeduba and Akoh, 2016; Leiva *et al.*, 2017). In this study, the method of wet heating with shortened reaction time at high temperature made provision for enhancing the formation of MR products than the dry method. Until now, different proteins, such as soy-bean (Qi *et al.*, 2009), whey protein (Jiménez-Castaño *et al.*, 2007) and rice protein (Li *et al.*, 2009) have been conjugated with different saccharides to improve functional properties. The modified proteins often showed better solubility, emulsifying properties (Zhu *et al.*, 2010) and antioxidant activity (Gu *et al.*, 2009; Lertittikul *et al.*, 2007), suggesting that well-controlled MR may be a good method for the BSF larvae protein modification.

Maillard reaction products (MRPs) prepared by protein and glucose conjugation have been known to significantly improve protein functionality (Leiva *et al.*, 2017). Previous studies have shown that BSF larvae (BSFL) conjugates have high antioxidant and enhanced techno-functional properties (Mshayisa and Van Wyk, 2021). Changes in the protein functional properties of edible insects according to three processes (grounded (G), defatted (D), and extracted (E)) were studied by Kim *et al.* (2020). However, there is no published information about the amino acid profile of the conjugated BSFL protein. Amino acid profile information is important for this study as it gives information about the quality of the proteins. When supplementing food products with insect-based protein and/or fractions, protein properties such as thermal stability, water and oil binding, amino acid profiles and foaming and emulsifying capacity are influential towards the final product (Bußler *et al.*, 2016).

Therefore, the purpose of this study was to characterise the BSFL protein, conjugate the protein with glucose and determine the amino acid profile before and after conjugation via MR. In order to elucidate conformational changes in the chemical structure, protein degradation was monitored in terms of scanning electron microscopy (SEM). Furthermore, thermal analysis techniques were studied to obtain information on the molecular structure and to detail conformational modifications that occur during conjugation. Universal attenuated total reflectance Fourier-transform infrared spectroscopy (UATR-FTIR) technique along with principal component analysis (PCA) was used to probe changes in the protein structure.

2. Materials and methods

Materials

BSFL supplied by AgriProtein (Cape Town, South Africa) were cleaned by blanching at 100 °C for 2 min to prevent browning and stored at -80 °C until further processing. The insect was ground in a blender (Bamix, Checkers, Cape Town, South Africa) and freeze-dried (Wizard 2.0, SP Scientific, Johannesburg, South Africa) to obtain a more stable product.

Glucose, acetonitrile (LC grade), methanol (LC grade), borate buffer, ethylenediaminetetraacetic acid (EDTA), tris-HCl, o-phthaldialdehyde (OPA), fluorenyl-methyl chloroformate (FMOC) reagents and a standard solution mixture of 18 amino acids were obtained from Sigma-Aldrich (Aston Manor, South Africa), all were of analytical grade unless stated otherwise. Amber vials and caps were purchased from Merck (Johannesburg, South Africa). Chemicals for protein extraction and for adjusting the pH of the solutions were NaOH and HCl purchased from Merck. Solutions, prepared using deionised water (Milli-Q system) with a resistivity of 18.2 MΩ.cm, and reagents were stored under conditions that prevented deterioration or contamination.

Dried insect flour preparation

Freeze-dried larvae samples were defatted at room temperature using hexane and isopropanol (ratio 3:2). One part of freeze-dried insect powder and five parts of the solvent mixture was stirred on a magnetic stirrer (Lasec, Cape Town, South Africa) for 2 h. Following sedimentation of the solids, the solvent-fat-mixture was decanted. The procedure was repeated twice. Residual solvent was removed by evaporation in the fume hood overnight. Subsequent fine grinding of the defatted samples using a mortar and pestle (Lasec) for a complete fine powder, and sieving to remove the integument, produced defatted BSF flour.

Protein extraction

Protein extraction was conducted according to the method of Azagoh *et al.* (2016) with slight modifications. Proteins were extracted from the defatted BSF larvae flour by applying solubilisation of 5 g of the defatted sample into 200 ml water adjusted to pH 10 with 1 N NaOH solution. The magnetic stirrer (Lasec) was used to stir the mixture on a hot plate (Lasec) at a speed created to halt the formation of a vortex, at 45 °C for 1 h. The pH was kept at 10 throughout the mixing period. After stirring, distilled water at pH 10 adjusted by NaOH, was added to reach 250 ml of solution. The mixture was centrifuged (Thermo Electron Corporation, Johannesburg, South Africa) at 10,000×*g* for 30 min at room temperature. The pellets were freeze-dried (Wizard 2.0, SP Scientific) before use for the upcoming experiments. The protein content was determined using the Dumas method (Leco Africa, Cape Town, South Africa) with a protein-to-nitrogen conversion factor of 5.60 (Janssen *et al.*, 2017).

Preparation of protein-glucose conjugates

MRPs were prepared in accordance with the modified method of Mshayisa (2016) and Vhangani and Van Wyk (2013). BSFL protein (2.0 g) and glucose (1.0 g) were dissolved in 100 ml of 0.1 M Tris-HCl buffer at pH 9. The samples were transferred into 250 ml Schott bottles and heated for 30, 60, 90 and 120 min at 50, 70 and 90 °C in a water bath, respectively. Samples of protein without glucose were subjected to the same treatment and were prepared as the control. After heating, the resulting MRPs were immediately cooled in an ice bath. MRP solutions were subject to pH measurement. The solutions were subsequently freeze-dried to obtain the products in powder form. The powders were stored in air-tight screw-capped glass bottles at -80 °C until analysis.

Protein content

Crude protein content was determined using Dumas (TruSpec™ Leco Carbon/Hydrogen/Nitrogen Series, Leco Africa) which was calibrated with EDTA (AOAC, 2000), using a protein-to-nitrogen conversion factor of 5.60, as recommended by Janseen *et al*. (2017).

Amino acids analysis

Amino acids were determined on protein extracts, heated proteins and protein-glucose conjugates according to the method of Jajić *et al.* (2013) with slight modifications.

A fine powder sample of 0.5 g was weighed (equivalent to 10 mg nitrogen content) into a screw-capped test tube and 7 ml of 6 M HCl was added. The tubes were capped, and the samples were hydrolysed for 6 h at 110 °C. Samples were cooled to room temperature and evaporated to dryness using a Reacti-Therm™ (Thermo Fisher Scientific, Johannesburg, South Africa) heating/stirring module, at 70 °C under a stream of nitrogen. The residues were quantitatively transferred and made up to volume in 100 ml volumetric flasks using 0.1 M HCl. The solutions were filtered using 0.22 µm pore size cellulose membrane syringe filters (Sigma-Aldrich, Johannesburg, South Africa) into high-performance liquid chromatography (HPLC) vials.

The analysis was performed on an Agilent 1260 Infinity II liquid chromatography system (Chemetrix, Midrand, South Africa), equipped with a µ-degasser (G7111A), 1260 binary pump (G7111B), 1260 standard auto-sampler (G7129B), 1260 thermostated column compartment (G1316A), 1260 diode array and multiple wavelength detector (G7117C), and a Zorbax Eclipse-AAA column (150 mm × 4.6 mm, i.d., particle size 5 µm; Chemetrix). The chromatographic conditions employed were in accordance with the Agilent method (Henderson *et al.*, 2000). Mobile phase A was acetonitrile:methanol:water (45:45:10, vol. %). The mobile phase B, consisted of 5.5 g of Na_2HPO_4 per 1 l of distilled water, adjusted to the pH 7.8 using 10 M NaOH solution. The gradient that was used is displayed in Table S1. The hydrolysed samples and solutions of the standard amino acid mixture were derivatised with OPA and FMOC using the autosampler programme for solution mixing and 0.5 µl of each sample were injected into a Zorbax Eclipse-AAA column at 40 °C, with detection at λ1=338 nm and λ2=262 nm. The separation was performed at a flow rate of 1 ml/min employing a solvent gradient (vol. %). This method was validated (results not shown).

Thermal gravimetric analysis

Thermal stability behaviour of the extracted protein, proteins heated alone and MRPs was analysed using the thermal gravimetric analysis (TGA) system (Perkin Elmer, TGA 7, Midrand, South Africa). To ensure the system was free from interparticle, heat and mass transfer resistances, the mass of the samples was retained within 10±0.2 mg and were carefully placed on the heating pan. The tests were conducted in the ramp mode of temperature range from 30 °C to 700 °C at a constant heating rate of 10 °C/min. Nitrogen carrier gas (flow rate of 20 ml/min) was used to avoid thermo-oxidative degradation.

Differential scanning calorimetry

The differential scanning calorimetry (DSC) profile of the samples was evaluated using a Perkin-Elmer DSC thermal analysis system. The samples (3-5 mg) were placed in hermetically sealed aluminium pans, heated from 30 to 300 °C at a constant rate of 10 °C/min with a constant purging of nitrogen at a rate of 20 ml/min. A sealed empty aluminium pan was used as a reference. Thermal transitions

of samples were measured for the denaturation temperature. The transition temperature (T_{max}) and total transition enthalpy changes (ΔH) were recorded.

Universal attenuated total reflectance Fourier-transform infrared spectroscopy

FTIR can be utilised to identify functional groups present in solids. The samples were analysed using a Perkin Elmer FTIR equipped with a (UATR) polarisation accessory. A total of 32 scans were conducted at a resolution of 4 cm^{-1} in the range of 4,000-600 cm^{-1} and saved in JCAMP-DX-format, one of many adapted formats for further statistical treatment by various software. Prior to data collection of each sample, the background air spectrum, water vapour and CO_2 interferences were subtracted from these spectra. The UATR crystal was cleaned with acetone. Sample powders obtained by grinding in a mortar and pestle were placed directly covering the surface of the ATR crystal. After baseline correction and smoothing was performed using the Savitzky-Golay function on OriginPro 8.6 software for Windows® (Dell Technologies, Cape Town, South Africa), the spectrum data were imported to Unscrambler 11 software for Windows, to standardise the normal variations.

Statistical multivariate analysis: principal component analysis

This projection method uses only the most important principal components of the PCA, which are factors relating to sensor signals (Petrozzi, 2013). PCA calculation is based on a singular value decomposition of the data array of the fingerprint region of the FTIR spectrum. The first two scores of the PCA results were used to make a projection plot that provided a visual determination of the similarity among the fingerprints. The samples are in the wavelength space known as the variance, which is represented by the drawing of an ellipsoid around the sample. Unscrambler 11 for Windows was used for the PCA in this work.

Scanning electron microscopy

The SEM (Electron Microscopy Sciences, Hatfield, PA, USA) was employed to observe microstructure and morphologies of all samples which were mounted directly on aluminium specimen stubs with conductive double-sided adhesive carbon tabs (EM-Tec CT12, Innovative Microscopy Supplier, Somerset West, South Africa) prior coating. Specimens were coated with gold using a Polaron SC 515 Sputter Coater (Durban, South Africa). Digital images of topographical features of the samples were collected using a Quanta 200 FEG environmental SEM (Durban, South Africa) operated in the high vacuum/secondary electron imaging mode at an accelerating voltage of 10 kV. The magnification of the images ranged from 150× to 2,000×. The images were used to find the difference in the structure of the samples.

3. Results and discussion

Amino acids

The BSFL protein extracted from the defatted larvae according to Azagoh's method was analysed for the protein content using the Dumas method. The value obtained (67±0.78% (n=3)) had increased by 17% from the initial Dumas figure of 50±0.54% (n=3) acquired prior to protein extraction (not shown). The amino acid profile of this BSFL protein, analysed by HPLC, is shown in Table 1.

Although the approximation of protein is determined, amino acid compositions show the quality of the protein. Tryptophan, cysteine and proline analyses were not included in the analysis due to their correlation coefficient being lower than the standard value, 0.9999. BSFL protein (Table 1) displays an amino acid profile comparable to casein and soybean, with the presence of both essential and non-essential amino acids, with a similar amino acid profile reported by Azagoh *et al.* (2016) on mealworm protein extracts and by Huang *et al.* (2019) on BSF (*Hermetia illucens*) in which two drying methods (conventional and microwave drying) were compared.

The BSFL protein contained all the essential amino acids in quantities generally higher than those necessary for humans (FAO, 2013). The sum of essential amino acids (EAA) was comparable to that of soy-bean protein, and slightly lower than that of casein, as reported by Young and Pellet (1991). The valine (123 mg/g protein) was the predominant essential amino acid, while glutamic acid content (152 mg/g protein) was found to be the highest non-essential amino acid. According to Phat *et al.* (2016), the high levels of glutamic acids are responsible for the special flavour and taste, while valine is responsible for muscle growth and tissue repair (Bishop *et al.*, 2020). The total sulphur amino acid content (methionine) was 80 mg/g which was higher than the content of FAO standard mode for older children, adolescents and adults (23 mg/g). Results reported by Huang *et al.* (2019) were lower for both conventional (38 mg/g) and microwave drying (34 mg/g). The aromatic amino acids (threonine and histidine) were similar to the results reported by Huang *et al.* (2019)) and the required amounts of FAO. In addition, the valine, which has multiple roles in protein interaction, tissue growth and repair (Phat *et al.*, 2016), was more than three times the requirement of FAO (40 mg/g).

The concentration of the nine essential amino acids was higher in BSFL than the recommended daily intake. This included lysine, methionine and valine which are limiting amino acids in the human diet. Only isoleucine and phenylalanine were 5 mg/g lower than the FAO recommended value. Limiting amino acids are not synthesised by mammals and are therefore essential in the

Table 1. Amino acid (AA) profile of protein extract from defatted black soldier fly larvae (BSFL) (current study), casein and soybean protein (Young and Pellet, 1991) and the recommended dietary allowance for human nutrition from Food Agricultural Organization (FAO), 2013.[1]

Amino acid (mg/g protein)	BSFL protein (current study)	Casein	Soybean	FAO 2013 (mg/g protein)[2]
Essential amino acids (EAA)				
Histidine	47.23±0.88	32	25	16
Isoleucine	25.37±0.52	54	47	30
Leucine	82.53±0.41	95	85	61
Lysine	45.03±1.44	85	63	48
Methionine	79.17±0.85	35	24	23
Phenylalanine	32.10±0.94	111	97	41
Threonine	45.57±0.42	42	38	25
Tryptophan	-	-	-	7
Valine	121.93±1.36	63	49	40
Sum of EAA	477.93	517	428	291
Non-essential amino acids				
Alanine	72.17±0.62			
Arginine	55.63±0.52			
Aspartic acid	119.23±0.56			
Glutamic acid	151.40±0.99			
Glycine	104.00±0.82			
Serine	58.27±0.38			
Tyrosine	63.90±0.14			
Sum of AA	1,102.53			

[1] Mean values ± standard deviation (n=3).

[2] The dietary allowance as reported by FAO, 2013; for adult maintenance in mg/g protein.

human diet as they are indispensable nutrients, found in plant food sources and gelatine. With BSFL protein showing a high concentration of these amino acids, it is, therefore an ideal protein source.

The protein extract was used in the conjugation process with glucose using MR. The amino acid composition of the BSF proteins (unheated), heated-treated BSF proteins and conjugates is depicted in Table 2, 3 and 4, respectively. The sum of the essential amino acids appears in Figure 1. Compared to the protein amino acid composition, MR caused a decrease in the amino acid content in conjugates (Figure 1B), similarly to those observed by Gu *et al.* (2010) and Liu *et al.* (2016) on casein-glucose and whey protein isolate-glucose, respectively. The decreased amino acid content caused by conjugation of namely, histidine, valine and aspartic acid went from 16.50 to 4.60 mg/g, 16.50 to 4.6 mg/g, 24.50 to 6.13 mg/g, respectively (Table 2). The reduction of the available amino acid group is attributed to the binding of protein and sugar during glycation. Overall, heat treatment results in the decrease of amino acids, in both heated protein (Figure 1A) and conjugates (Figure 1B). Amino acid distribution is modified by all heating times, especially conjugates heated for 120 min at 90 °C (Figure S2D). This indicates that heating at a higher temperature for a longer period induces interactions of free amino acids. This is due to the fact that at high heating temperature, the conjugation reaction is faster since the proteins undergo considerable unfolding to conjugate (Liu *et al.*, 2016). The decrease in the amino acid content indicates that most proteins have reacted with the glucose under the employed heating conditions (Liu *et al.*, 2014). When the protein is heated alone, the alteration of the amino acid levels appears to cause a notable decrease of lysine content, considered the most reactive amino acid for the MR. Other amino acids displayed significant (P<0.05) decreases, namely, phenylalanine, alanine and tyrosine (Table 2). Similar results were reported by Zhang *et al.* (2012) from β-conglycinin and dextran conjugation. Supplementary Figure S1 shows the amino acid profiles of the protein extract (S1A), and heated proteins at the different temperatures and times; and Figure S2 the protein extract (Figure S2A), and MR products (Figure S2B) also at different temperatures and times in the form of bar graphs.

After 50 °C treatment, the amino acids declined for both BSF proteins and conjugates but not significantly (P>0.05) for the conjugates (Figure 1B). Although these amino

Table 2. Amino acid profile of the black soldier fly (BSFL) proteins (control), heated black soldier fly proteins and conjugates heated for 30, 60, 90 and 120 min at 50 °C.[1]

Amino acids (mg/g protein)	Control (unheated)	BSFL protein heated at 50 °C				Conjugates heated at 50 °C			
		30 min	60 min	90 min	120 min	30 min	60 min	90 min	120 min
Histidine	46.23±0.88^{f}	16.50±0.26^{e}	10.33±0.06^{d}	9.77±1.01^{d}	3.60±0.36^{a}	4.60±0.53^{ab}	5.47±1.36^{bc}	6.27±1.62^{c}	3.93±0.60^{ab}
Isoleucine	25.37±0.52^{c}	9.43±0.21^{b}	4.57±0.40^{a}	4.50±0.44^{a}	4.13±0.90^{a}	3.63±1.18^{a}	5.13±1.01^{a}	3.83±1.39^{a}	3.77±1.50^{a}
Leucine	82.53±0.41^{f}	72.27±0.47^{e}	61.40±0.53^{d}	26.13±0.90^{b}	13.87±0.15^{a}	27.40±2.16^{b}	30.33±1.53^{c}	27.63±2.80^{b}	32.63±1.58^{c}
Lysine	45.03±1.44^{f}	32.43±0.15^{e}	16.93±0.81^{d}	14.50±0.30^{c}	1.60±0.53^{a}	6.00±1.00^{b}	6.57±0.81^{b}	6.77±1.37^{b}	3.00±1.91^{a}
Methionine	79.17±0.85^{c}	9.50±0.10^{b}	4.80±0.20^{a}	4.40±0.26^{a}	4.03±0.90^{a}	3.33±1.53^{a}	3.80±1.74^{a}	3.63±1.59^{a}	3.63±1.59^{a}
Phenylalanine	32.10±0.94^{e}	21.60±0.20^{d}	14.73±0.25^{c}	14.13±0.49^{c}	4.63±0.78^{a}	9.70±1.47^{b}	7.93±6.14^{ab}	8.30±1.57^{ab}	5.50±1.50^{ab}
Threonine	45.57±0.42^{e}	21.43±0.21^{d}	13.77±0.21^{c}	7.03±0.95^{b}	2.70±0.26^{a}	4.03±1.00^{a}	3.70±0.36^{a}	6.63±1.58^{b}	3.83±1.70^{a}
Valine	121.93±1.36^{f}	20.50±0.10^{c}	10.10±0.10^{b}	9.67±0.84^{b}	3.43±0.32^{a}	4.00±1.00^{a}	4.93±1.10^{a}	4.50±1.32^{a}	3.57±0.25^{a}
Sum of EAA	477.93	203.66	136.86	83.2	38.16	63.29	68.4	69.33	60.22
Alanine	72.17±0.62^{d}	20.50±0.10^{c}	10.10±0.10^{b}	9.67±0.84^{b}	3.43±0.32^{a}	4.00±1.00^{a}	4.93±1.10^{a}	4.50±1.32^{a}	3.57±0.25^{a}
Arginine	55.63±0.52^{f}	21.73±0.32^{e}	9.57±0.15^{d}	9.03±0.91^{d}	1.63±0.47^{a}	4.23±1.08^{bc}	5.77±1.97^{c}	3.30±1.54^{ab}	2.47±1.65^{ab}
Aspartic acid	119.23±0.56^{g}	24.50±0.10^{f}	12.47±0.25^{e}	10.03±1.00^{d}	2.60±0.36^{a}	6.13±0.81^{c}	5.43±0.51^{bc}	4.03±1.05^{ab}	3.63±1.55^{a}
Glutamic acid	151.40±0.99^{f}	28.73±0.25^{e}	11.23±0.25^{d}	8.90±1.01^{c}	1.07±0.25^{a}	4.50±2.29^{b}	10.30±1.82^{cd}	8.27±1.62^{c}	8.40±1.44^{c}
Glycine	104.00±0.82^{e}	35.53±0.47^{d}	15.40±0.36^{c}	15.03±0.65^{c}	1.93±0.06^{a}	7.43±1.40^{b}	7.27±0.64^{b}	6.43±1.50^{b}	6.57±0.59^{b}
Serine	58.27±0.38^{f}	35.37±0.35^{e}	18.90±0.10^{d}	10.40±0.53^{c}	0.73±0.14^{a}	9.07±0.90^{c}	9.90±1.15^{c}	9.70±1.47^{c}	7.17±1.89^{b}
Tyrosine	63.90±0.14^{e}	17.20±0.26^{d}	7.53±0.31^{c}	1.27±0.25^{a}	0.90±0.66^{a}	3.80±0.60^{b}	6.13±2.39^{c}	1.87±1.10^{a}	1.97±1.27^{a}
Sum of AA	1,102.53	387.22	222.06	147.53	50.45	102.45	118.13	107.43	94

[1] Values are the mean ± SD (n=3); values with a different superscript in the same row indicate significant differences (P<0.05).

Table 3. Amino acid profile of the black soldier fly (BSFL) proteins (control), heated black soldier fly proteins and conjugates heated for 30, 60, 90 and 120 min at 70 °C.[1]

Amino acids (mg/g protein)	Control (unheated)	BSFL protein heated at 70 °C				Conjugates heated at 70 °C			
		30 min	60 min	90 min	120 min	30 min	60 min	90 min	120 min
Histidine	46.23±0.88^{f}	5.34±0.15^{b}	3.57±0.25^{a}	3.13±0.99^{a}	3.13±0.96^{a}	2.13±0.15^{a}	2.73±0.25^{a}	2.79±1.13^{a}	2.11±1.34^{a}
Isoleucine	25.37±0.52^{c}	5.48±0.09^{c}	5.23±0.25^{c}	4.47±0.46^{bc}	3.80±1.44^{ab}	2.81±0.09^{a}	3.37±0.25^{ab}	2.51±0.45^{a}	2.87±1.44^{a}
Leucine	82.53±0.41^{f}	26.90±0.36^{c}	25.33±0.57^{c}	25.27±1.70^{c}	25.57±1.25^{c}	30.64±0.36^{d}	18.73±0.57^{b}	18.03±1.71^{b}	14.42±1.25^{a}
Lysine	45.03±1.44^{f}	4.73±0.31^{cd}	3.67±0.32^{abc}	4.40±1.04^{bcd}	2.17±0.47^{a}	5.47±0.31^{d}	3.50±0.35^{abc}	3.00±1.04^{ab}	2.39±0.47^{a}
Methionine	79.17±0.85^{c}	3.80±0.20^{bc}	4.20±1.06^{c}	3.90±1.13^{bc}	3.96±1.03^{bc}	2.23±0.21^{bc}	2.63±1.05^{abc}	1.69±1.13^{a}	1.25±1.02^{a}
Phenylalanine	32.10±0.94^{e}	5.43±0.40^{d}	5.13±0.32^{cd}	4.73±1.10^{abcd}	4.97±0.84^{bcd}	3.40±0.40^{a}	3.73±0.32^{abc}	3.34±1.10^{a}	3.60±0.84^{ab}
Threonine	45.57±0.42^{e}	20.53±0.31^{g}	16.63±0.91^{f}	14.20±1.31^{e}	12.30±0.61^{d}	7.57±0.32^{c}	3.93±0.95^{b}	2.05±1.31^{a}	2.40±0.61^{a}
Valine	121.93±1.36^{f}	3.97±1.05^{c}	3.33±1.01^{abc}	3.77±1.37^{c}	3.50±0.26^{abc}	3.67±1.04^{bc}	2.17±1.03^{abc}	1.60±1.37^{ab}	1.44±0.26^{a}
Sum of EAA	477.93	76.18	67.09	63.87	59.4	57.92	40.79	35.01	30.48
Alanine	72.17±0.62^{d}	2.33±0.42^{ab}	2.70±0.70^{ab}	3.00±1.00^{b}	1.67±0.49^{ab}	2.83±0.40^{ab}	2.80±0.70^{ab}	1.67±1.01^{ab}	1.57±0.49^{a}
Arginine	55.63±0.52^{f}	5.17±0.76^{d}	3.87±0.61^{c}	3.27±0.64^{bc}	2.57±0.40^{ab}	1.70±0.75^{a}	3.67±0.60^{bc}	2.56±0.59^{ab}	3.06±0.40^{bc}
Aspartic acid	119.23±0.56^{g}	6.17±0.38^{d}	6.90±1.15^{d}	5.50±0.87^{cd}	2.13±2.06^{a}	4.73±0.35^{bcd}	2.73±1.10^{ab}	3.84±0.87^{abc}	3.03±2.06^{ab}
Glutamic acid	151.40±0.99^{f}	2.30±0.30^{a}	5.47±1.36^{b}	4.10±0.85^{ab}	2.83±1.53^{a}	2.33±0.31^{a}	3.63±1.35^{ab}	2.87±0.85^{a}	2.81±1.53^{a}
Glycine	104.00±0.82^{e}	6.30±0.61^{c}	5.80±0.46^{c}	5.23±0.68^{bc}	1.93±2.06^{a}	5.70±0.61^{c}	4.43±0.45^{bc}	4.18±0.68^{bc}	3.25±2.06^{ab}
Serine	58.27±0.38^{f}	2.53±0.68^{b}	1.90±0.36^{ab}	1.37±0.32^{a}	1.43±0.40^{a}	5.93±0.70^{d}	4.53±0.35^{c}	1.57±0.32^{a}	1.50±0.40^{a}
Tyrosine	63.90±0.14^{e}	4.40±0.40^{c}	3.67±0.72^{bc}	2.13±0.71^{a}	4.07±1.04^{c}	12.53±0.40^{e}	10.93±0.75^{d}	2.67±0.71^{ab}	2.52±1.06^{ab}
Sum of AA	1,102.53	105.38	97.4	88.47	76.03	93.67	73.51	54.37	48.22

[1] Values are the mean ± SD (n=3); values with a different superscript in the same row indicate significant differences (P<0.05).

Table 4. Amino acid profile of the black soldier fly (BSFL) proteins (control), heated black soldier fly proteins and conjugates heated for 30, 60, 90 and 120 min at 90 °C.[1]

Amino acids (mg/g protein)	Control (unheated)	BSFL protein heated at 90 °C				Conjugates heated at 90 °C			
		30 min	60 min	90 min	120 min	30 min	60 min	90 min	120 min
Histidine	46.23±0.88^{f}	5.64±0.51^{d}	3.43±0.32^{c}	2.33±1.33^{bc}	3.37±0.60^{c}	2.34±0.51^{bc}	1.43±0.31^{ab}	1.11±0.66^{ab}	0.90±0.85^{a}
Isoleucine	25.37±0.52^{c}	5.53±0.05^{d}	4.30±1.82^{bcd}	3.48±1.98^{abcd}	4.53±0.42^{cd}	2.77±0.06^{abc}	2.00±1.82^{ab}	1.87±1.96^{ab}	1.41±0.43^{a}
Leucine	82.53±0.41^{f}	26.47±1.10^{de}	25.03±1.08^{d}	25.27±1.70^{d}	21.07±0.89^{c}	28.05±1.10^{e}	14.18±1.08^{b}	11.16±1.69^{a}	10.12±0.89^{a}
Lysine	45.03±1.44^{f}	5.20±0.92^{cd}	3.97±0.70^{bc}	4.03±1.67^{bc}	2.50±1.04^{ab}	6.83±0.92^{d}	5.01±0.70^{cd}	2.92±1.68^{abc}	0.83±1.04^{a}
Methionine	79.17±0.85^{c}	3.36±0.94^{bc}	4.20±1.06^{c}	3.90±1.13^{c}	3.96±1.03^{c}	2.82±0.94^{abc}	1.92±1.06^{ab}	1.22±1.13^{a}	1.89±1.03^{ab}
Phenylalanine	32.10±0.94^{e}	6.18±0.92^{cd}	4.87±0.71^{bc}	4.73±1.10^{bc}	4.67±0.76^{bc}	6.83±0.92^{d}	3.76±0.71^{b}	1.54±1.11^{a}	2.12±0.76^{a}
Threonine	45.57±0.42^{e}	7.60±1.04^{de}	8.63±1.19^{e}	5.87±1.03^{cd}	8.20±1.59^{e}	4.62±1.04^{bc}	3.72±1.18^{b}	1.11±1.03^{a}	2.80±1.58^{ab}
Valine	121.93±1.36^{f}	3.37±2.01^{a}	1.13±0.81^{a}	3.19±2.33^{a}	2.48±1.87^{a}	6.70±2.00^{b}	4.36±0.82^{ab}	2.82±2.35^{a}	2.13±1.86^{a}
Sum of EAA	477.93	63.35	55.56	52.8	50.78	60.96	36.38	23.75	22.2
Alanine	72.17±0.62^{d}	7.07±2.10^{b}	5.78±0.69^{b}	3.00±1.00^{a}	1.34±0.58^{a}	1.99±1.49^{a}	2.52±0.71^{a}	2.06±1.00^{a}	1.25±0.57^{a}
Arginine	55.63±0.52^{f}	4.40±1.97^{c}	3.87±0.61^{bc}	3.27±0.64^{bc}	2.57±0.40^{abc}	3.69±1.43^{bc}	2.69±0.61^{abc}	2.28±0.64^{ab}	1.44±0.40^{a}
Aspartic acid	119.23±0.56^{g}	6.14±0.40^{c}	2.76±0.67^{ab}	4.73±2.19^{bc}	1.03±0.20^{a}	5.78±0.30^{c}	4.65±0.67^{bc}	3.00±2.19^{ab}	2.72±0.19^{ab}
Glutamic acid	151.40±0.99^{f}	3.27±1.94^{abc}	5.47±1.36^{c}	4.34±0.57^{bc}	3.08±1.95^{abc}	2.28±1.41^{ab}	1.39±1.35^{a}	1.42±0.58^{a}	2.22±1.95^{ab}
Glycine	104.00±0.82^{e}	8.40±1.64^{cd}	11.17±1.26^{d}	8.34±2.53^{cd}	3.07±2.10^{ab}	6.30±1.62^{bc}	5.77±1.25^{abc}	2.93±2.54^{ab}	2.37±2.10^{a}
Serine	58.27±0.38^{f}	3.25±1.22^{b}	2.54±1.39^{ab}	1.43±0.40^{a}	1.37±0.32^{a}	5.76±0.95^{c}	5.29±1.39^{c}	2.87±0.40^{ab}	1.87±0.32^{ab}
Tyrosine	63.90±0.14^{e}	3.67±1.63^{a}	3.13±1.46^{a}	1.89±0.34^{a}	3.64±1.77^{a}	13.87±1.15^{c}	9.81±1.46^{b}	3.56±0.34^{a}	2.13±1.77^{a}
Sum of AA	1,102.53	99.55	90.28	79.8	66.88	100.63	68.5	41.87	36.2

[1] Values are the mean ± SD (n=3); values with a different superscript in the same row indicate significant differences (P<0.05).

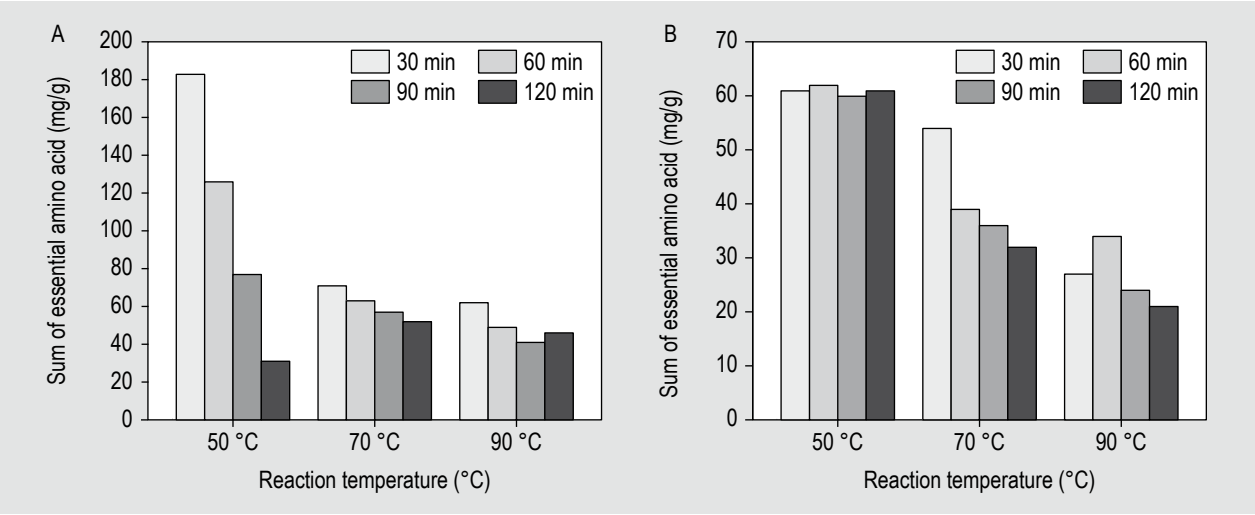

Figure 1. Sum of essential amino acids of the heated proteins (A) and in Maillard reaction conjugates (B) as a function of reaction temperature.

groups participate in the initial stage of MR by reacting with carbonyl groups to form a Schiff base, a longer heating period and higher temperature results in the degradation and Amadori rearrangement groups formation (Sun *et al.*, 2006). It was also clear that the reactivity of the amino groups at 50 °C was less than at 90 °C (Figure 1B). Similar results were reported previously, where a decrease in the amino acid content of the conjugates resulted due to the MRPs formation (Jiménez-Castaño *et al.*, 2007) during the glycation of whey protein and dextran.

Figure 1 focused on identifying the impact of temperature in the heated proteins and MR conjugates. As the temperature increased, the content of the essential amino acids decreased. Again, this is expected as the amino acids are consumed during the MR. It can be concluded that as the temperature and heating time are increased, the essential amino acids are reduced.

The EAA profile of the BSF protein (Table 1) revealed that the EAA levels were comparable with those of FAO amino acid reference (FAO, 2013) recommended for human nutrition. Amino acid composition determines the protein's nutritional value. Therefore, it can be concluded that BSFL protein could be an alternative source of essential amino acids for human nutrition.

Thermal gravimetric analysis

The weight loss curve obtained by TGA for MRPs at three different temperatures, 50, 70 and 90 °C for 30 min, 60 min, 90 min and 120 min, are presented in Figure 2, respectively. The TGA curves show the remaining weight between temperatures of 50 to 700 °C. Additionally, supplementary Figure S3 and S4 display the TG (thermal gravimetric) and Differential Thermogravimetric (DTG) curves of the non-heated protein and the MRP at time zero, correspondingly. The initial mass degradation step at ~50 to 150 °C indicates the evaporation of moisture in the samples. For the heated proteins (Figure S4), the mass loss occurring in the range of ~250-550 °C may be associated with polypeptide decomposition. These TGA curves are similar to the results reported by Huang *et al.* (2019) for the BSFL dried flours with higher decomposition temperature which may be associated with polypeptides.

In terms of the mass losses of the MRPs (Figure 2), two stages of decomposition were observed, when compared to the heated proteins (Figure S4). The first stage is the loss of the bound water and some volatile substances in the glycosylated products between ~50 and 200 °C. The drop in mass occurred at a higher temperature than in the case of the proteins (Figure S5), possibly indicating a slightly stronger bonding between the volatiles and conjugated products. The weight loss in the conjugates is slightly higher than in the case of the proteins. In the second stage of the decomposition, between temperatures of ~250 to 550 °C, the percentage weight decreased due to the decomposition of the glycation products and MR intermediates, with the pyrolysis of some other macromolecules; after 550 °C, ash and other residues formed 35% of the total. The weight loss percentage of the protein heated alone is lower than that of the MRPs. This shows that the MRPs has larger molecules due to the protein and glucose molecule attachment, this observation is clearly shown in Supplementary material Figure S4.

These results are in close agreement with those reported by (Muley *et al.,* 2018) who studied the thermal decomposition of chitosan from prawn shell waste and its conjugation with cutinase. It was observed that a higher temperature was required to decompose the bound water on the MRP samples, compared to heated proteins. Comparing the heating times and temperatures within Figure 2 with Figure S5, there was no difference between protein heated alone curves. However, Figure 2C showed a difference between 30, 60, 90 and 120 min. However, other researchers have reported more than two steps of mass loss. However, these samples were subjected to different drying methods, that is, conventional and microwave drying (Huang *et al.*, 2019; Wasko *et al.*, 2016).

Comparing all the results as shown in Figure 2 and Supplementary Figure S5, the decomposition temperature depends markedly on the sample, in this case on how long and at what temperature they were heated. Increasing the heating time and the temperature is accompanied by an increase in the decomposition temperature of the MRPs, meaning the non-heated protein will have a lower decomposition temperature than the MRPs.

The best preparation conditions of BSFL protein:glucose glycation, was the reaction temperature at 90 °C for 120 min, showing ~40% residue remaining, which demonstrates that the sample had larger molecules due to the attachment of the protein and glucose molecules and better heat stability than the original sample.

Differential scanning calorimetry

Endothermic peaks at 90, 240, 320 and 400 °C were observed in the DSC profiles for the heated proteins (Figure S6), possibly due to melting peptides. The resultant increase in enthalpy, a phenomenon that is indirectly proportional to the increase in heating time, proves that, after higher heating time, the proteins are more stable. More energy will be required to break down the polypeptides, a phenomenon that is in accord with TGA analysis. The longer reaction time (heating time) during MRP preparation increased the thermal stability of the MRPs, while higher reaction temperature decreased the thermal stability. Furthermore, the enthalpy of MRPs gradually decreased with the increasing reaction temperature of the treatments (Figure 3). These findings are in agreement with the results reported by Muley *et al.* (2018) who studied chitosan of the prawn shell waste and cutisane glycation. During the heating, it is possible that the initially ordered structure of the BSFL protein is gradually destroyed.

Nuthong *et al.* (2009) confirmed that the increase in denaturation temperature might be as the result of the MR inducing the cross-linking of molecules. After the conjugation reaction, the magnitude of the enthalpy was

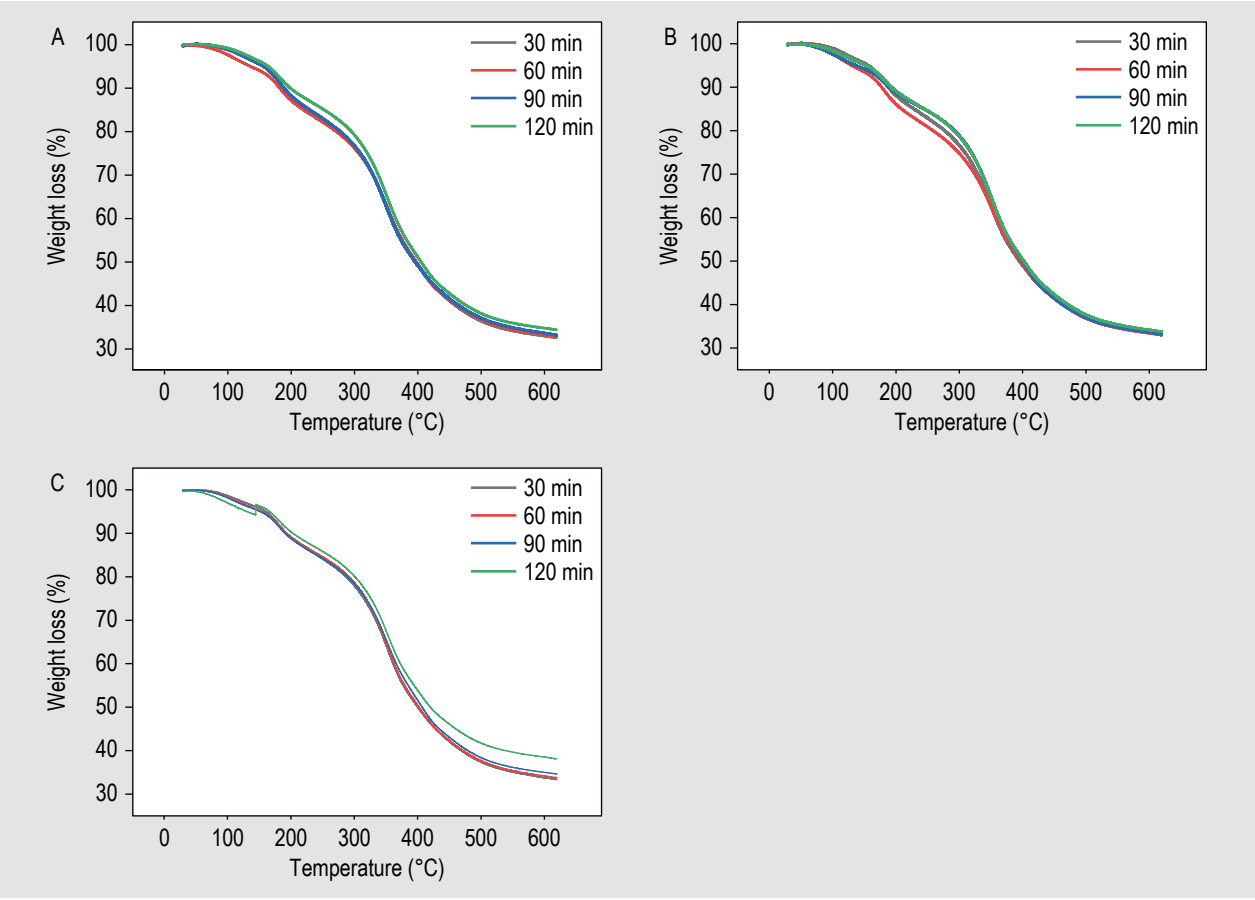

Figure 2. Thermal gravimetric analysis of the protein-glucose conjugates heated for 30, 60, 90 and 120 min at (A) 50 °C, (B) 70 °C and (C) 90 °C.

reduced, this may be attributed to the intermolecular forces of the BSFL samples being disrupted when they are covalently bound to carbohydrate molecules. In accordance with this study, the steric spacers between the protein molecules may be reduced by the glucose molecules, enhancing the interactions of the hydrophobic binding sites which would promote aggregation.

Universal attenuated total reflectance Fourier-transform infrared spectroscopy

The FTIR bands are shown in Supplementary Figures S7 and S8 for 50, 70 and 90 °C by four different heating times (30, 60, 90 and 120 min) for heated proteins and MRPs, respectively. As the reaction with glucose progressed, the absorptions in the region of amide showed an increase in intensity with time, indicating that glucose molecules may have attached to the BSFL protein, forming a Schiff base compound with amine groups (Figure S8). When compared with the native protein, conjugates rendered low intensity on the amide regions. The two most important vibrational modes of amides are the amide 1 vibrations (1,600-1,700 cm^{-1}), primarily caused as the result of C=O bonds, and the amide II vibrations (1,510-1,580 cm^{-1}), which are caused by N-H bonds due to its deformation and due to the C-N bond stretches. During the heating process, the -OH group in the amino groups in BSFL proteins and glucose might be expected to be consumed. Researchers found the intensity of the bands at 1,600-1,400 cm^{-1} gradually decreasing during the conjugation reaction between soy protein isolate (SPI) and carboxyl methylcellulose (CMC) (Su *et al.*, 2009). Gu *et al.* (2010) also observed that NH_2 and other functional groups, mainly the functional groups in lysine, may be decreased, whereas the amount of Maillard products, such as the Schiff bases (C=N), Amadori compound (C=O), and pyrazines (C-N), may be increased. This finding may be supported by the lower amino acid content (of arginine, lysine and histidine) of the MRPs formed during the MR (Table 2).

In addition, Figure S8C illustrates no change in the 1,033-601 cm^{-1} regions. Chang and Tanaka (2002) hypothesised that this could be as the result of MR completion, which, in spite of the fact that these bands cannot be categorised as a distinct functional group, they are also important in indicating a change in the protein structure, compared with proteins heated alone, this region increased in the glycated samples.

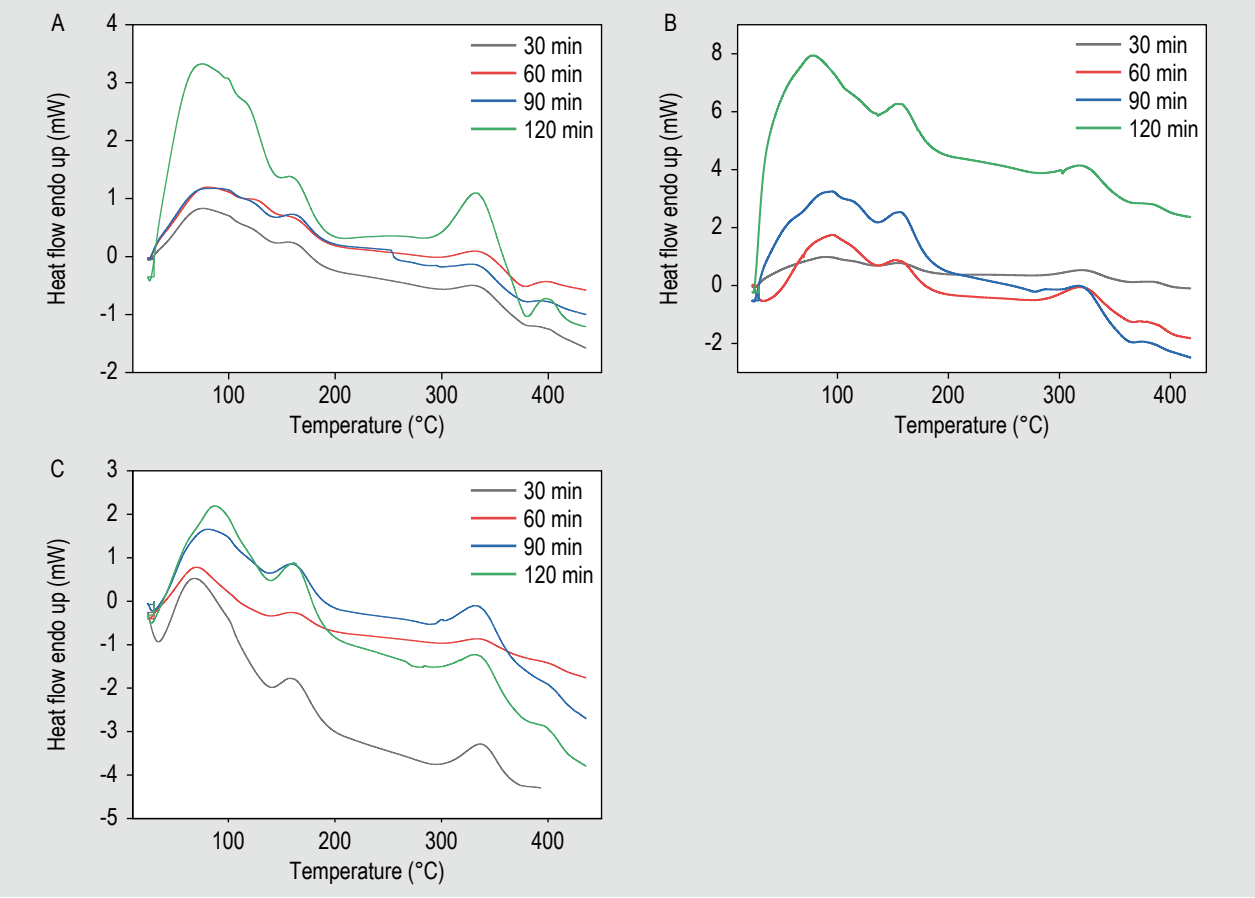

Figure 3. Differential scanning calorimetry of the protein-glucose conjugates heated for 30, 60, 90 and 120 min at (A) 50 °C, (B) 70 °C and (C) 90 °C.

As a result, it can be presumed that complicated aggregation or cross-linking may have occurred between the glycated samples. Additionally, due to increasing the reaction time and temperature, the free amino groups of the conjugates decreased quickly (Table 2). The FTIR results showed that the glucose had attached to the BSFL protein.

Principal component analysis

Due to the small changes to spectral bands for easily discerning between heating times and temperatures, a multivariate statistical approach was required for the FTIR analysis to notice the spectral changes, that is, a statistical method that is used to discriminate between samples shows the structure (the loadings) and systematic separation or outliers (the score plot). PCA of the entire data set of spectra was performed on the heated proteins and glycated samples (heated at 50, 70 and 90 °C for 30, 60, 90 and 120 min), applying the information supplied by the spectrum region where vibrational changes are associated with the major bands of carbohydrate, amide and hydroxyl appear (600-4,000 cm^{-1}). The dataset in the PCA is broken down into orthogonal components that explain the dataset and allows one to read only the differences in the spectra (Esbensen and Swarbrick, 2018). The spectra from the different samples clustered individually as shown by the PCA scores plots and the loadings plots show the coefficient of the linear combinations associated with each Principal Component (PC). This describes the greater source of variance which corresponds to the first principal axis of the ellipsoid. The central axis is the first principal component (PC1) and the second principal component (PC2), lies along a direction orthogonal to the first PC and along the direction of the second largest data set variance and the second main axis of the ellipsoid.

The score plot for the first two PCs from the FTIR normalised data of MRPs and heated proteins is shown in Figure 4. It was observed that 92% of data variances were explained by the analysis of the two principal components, 74% explained by the first and 18% in the second PC. The ellipse (known as Hotelling's T^2 ellipse) represents a 100-confidence interval around the model mean and is one criterion for detecting outliers. There are no outliers, characterised by excessively high scores, in the model space when PC1 and PC2 are jointly assessed. With reference to Figure 4, it can be seen that the MRPs at 90 and 70 °C, are in the far left of the plot, with the most negative score for

PC1, approximately -10 and -5, respectively and positive score for PC2, approximately 2.0 for both temperatures. The MRP samples move asymmetrically down the PC2, while the heated protein moves symmetrically from left to right along the PC1, from lower to higher temperature.

The PC1 positive axis is associated with the heated protein samples, while the positive axis of the PC2 is associated with MRPs. MRPs also contribute to PC1, but at the opposite end of the plot axis. For example, MRPs at 90 °C are approximately at -10 of the PC1 while the heated proteins at 90 °C are at +10 of the same axis. Therefore, samples that lie at approximately 180° from each other along the PC direction represent opposite features along the PC1, most likely due to the state of glycation varying through the course of the heat treatment. The clustering of the sample for protein heated alone is significantly different from the MRP samples showing that the observed differences were due to both glycation and heating. The clustering distance for the samples heated for 120 min was considered to be significant compared with that of the physical blend or for those samples exposed to lower temperatures and shorter heating times.

The loadings plot (Figure 4B) provides a further interpretation of the variable responsible for the separation. It is important to note that variables of large loadings lie away from the origin and variables of little importance lie near the origin. However, when assessing importance, it is mandatory to consider the proportions of the total explained variance along with each component, in this case, PC1 explains 74% and PC2 only 18%, then variables with large loadings in PC1 are much more important than those with large loadings in PC2. The most dominant variable in PC1 in region 1,441-1,609 cm^{-1} can be interpreted as when the band at 1,514 cm^{-1} increases or decreases. The PC1 (Figure 4B) separates according to the 3,292, 1,694 and 999 cm^{-1} regions (C=O), whereas PC2 is responsible for the separation according to regions 3,248, 1,550, 1,361 and 999 cm^{-1}.

From these results, it can be concluded that the UATR-FTIR managed to show differences in the structural changes of the protein heated alone and MRPs. It was also evident from the PCA (scores and loadings) that the major differences in the FTIR spectrum were caused by the protein region (amide I & II region), results complementing the results displayed by TGA and DSC.

Scanning electron microscopy

The molecular structures of food, too small to be inspected by the human eye, are provided by SEM information. The similarities and differences are displayed in the surface morphology of the non-heated BSFL samples (freeze-dried and defatted flours), the extracted protein and glucose (Figure S8). Initially, the particles are uneven, rigid and compact followed by more porous structures post defatting. These results are in agreement with reports on the surface morphology of wheat germ protein (Niu *et al.*, 2011), silver carp (Liu *et al.*, 2016) and chitin isolate extract from *H. illucens* by Wasko *et al.* (2016).

After conjugation, the large irregularly shaped particles (Figure 5), which originated from protein and sugar molecules (Figure S9) were observed. The glucose breaks the non-covalent bond of the protein during MR, resulting in unfolding and reduction of the protein molecule aggregation, resulting in the collapse of the protective layer on the material subjected to a higher temperature. Similar results of surface morphology were observed in MRPs of wheat germ protein (Niu *et al.*, 2011). It can be concluded

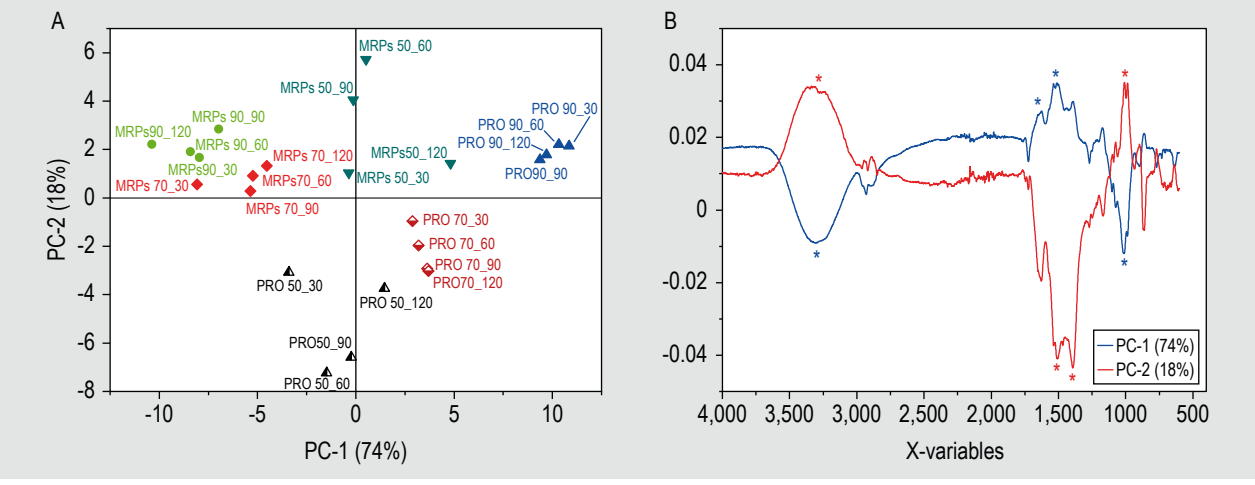

Figure 4. Principal component analysis scores of the full Fourier-transform infrared spectroscopy spectrum (A). Principal component 1 and principal component 2 are responsible for 74 and 18% variance, respectively of the heated proteins (Pro) and Maillard reaction products at 50, 70, 90 °C; (B) loadings plot principal component 1, responsible for 74% variance (blue) and principal component 2, responsible for 18% variance (red).

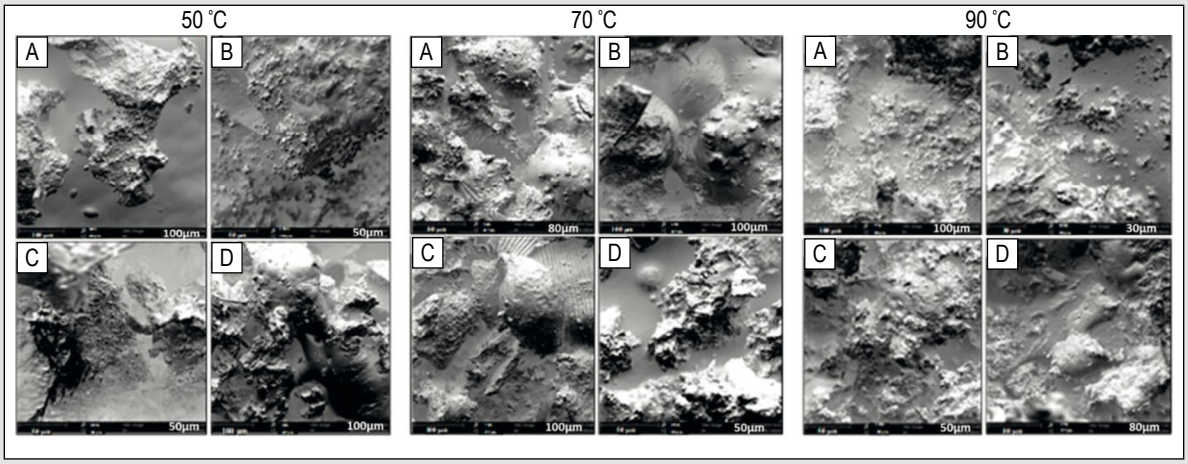

Figure 5. Scanning Electron Microscope photographs of Maillard reaction products at 50, 70 and 90 °C for (A) 30 min, (B) 60 min, (C) 90 min and (D) 120 min at 620 to 1,800× magnification.

that treatment at temperatures close to or higher than the denaturation temperature, 70 and 90 °C, resulted in the protein molecules unfolding. The two different surface morphologies described are (1) conventional dried BSFL flour, and (2) microwave dried BSFL (Huang *et al.*, 2019).

4. Conclusion

In conclusion, it was possible to obtain conjugates by MR between protein extracted from the BSFL flour and glucose. The amino acid levels of the protein were found to be comparable with those of FAO/WHO for human consumption. FTIR confirmed that an increase in the amount of glycation primes to an increase in the structural alteration of the protein. At the same time, the spectroscopic analysis of FTIR indicated that amide I and II were modified by MR. Upon comparing the samples in the FTIR through the PCA, it becomes evident that the protein has different properties on the PCs compared with the MRP samples. Both FTIR analysis and the DSC peak shifts of the MRPs testifies to the formation of the conjugates. In the case of TGA, longer reaction times improve the thermal properties and there was evidence that other products may have been formed. Compared with proteins heated alone, the MRPs showed similar thermal stability as displayed by the denaturation temperature of ~250-550 °C. As shown in the DSC analysis, the results of this study also demonstrate that the thermal stability of the protein was effectively enhanced by MR with glucose. Finally, the difference in surface morphology between the protein and conjugates was also determined by SEM. Therefore, the present results suggest that protein conjugated with glucose under MR conditions can be a promising way to improve the properties of the BSFL protein. The present study highlights that the stability and function of any insect glycoproteins can be improved in a simple and inexpensive manner.

Supplementary material

Supplementary material can be found online at https://doi.org/10.3920/JIFF2021.0017.

Table S1. Gradient elution program used for chromatographic separation of the amino acids.

Figure S1. Amino acid profiles of the protein extract, and heated proteins at 50, 70 and 90 °C for 30, 60, 90 and 120 min.

Figure S2. Amino acids in protein extract, Maillard reaction products at 50, 70 and 90 °C for 30, 60, 90 and 120 min.

Figure S3. Thermal gravimetric analysis and differential thermogravimetric of the non-heated black soldier fly larvae protein.

Figure S4. Thermal gravimetric analysis and differential thermogravimetric of the heated black soldier fly larvae protein(red) and Maillard reaction product (blue) both heated for 30 min at 50 °C.

Figure S5. Thermal gravimetric analysis of the heated protein for 30, 60, 90 and 120 min at 50, 70 and 90 °C.

Figure S6. Differential scanning calorimetry thermograms of the heated protein for 30, 60, 90 and 120 min at 50, 70 and 90 °C.

Figure S7. Fourier-transform infrared spectroscopy of heated proteins at 50, 70 and 90 °C for 30, 60, 90 and 120 min.

Figure S8. Fourier-transform infrared spectroscopy of Maillard reaction products at 50, 70 and 90 °C for 30, 60, 90 and 120 min.

Figure S9. Scanning electron microscope analysis of freeze-dried BSFL, defatted BSFL, BSFL extracted protein and glucose 320 to 650x magnification.

Acknowledgements

This work is based on the research supported by the National Research Foundation (NRF) of South Africa for the grant no. 116306, and the authors wish to thank the NRF, Agrifoods Technology Station, Mauerberger Foundation Fund and the Cape Peninsula University of Technology for financial and other support. Any opinion, finding and conclusion or recommendation expressed in this material is that of the author(s) and the NRF does not accept any liability in this regard. The authors declare that they have no conflict of interest.

Conflict of interest

The authors declare no conflict of interest.

References

Association of Official Analytical Chemists (AOAC), 2000. Official methods of analysis. AOAC, Washington, DC, USA.

Akhtar, M. and Ding, R., 2017. Covalently cross-linked proteins & polysaccharides: formation, characterisation and potential applications. Current Opinion in Colloid and Interface Science 52: 31-36.

Azagoh, C., Ducept, F., Garcia, R., Rakotozafy, L., Cuvelier, M.-E., Keller, S., Lewandowski, R. and Mezdour, S., 2016. Extraction and physicochemical characterization of *Tenebrio molitor* proteins. Food Research International 88: 24-31.

Balzan, S., Fasolato, L., Maniero, S. and Novelli, E., 2016. Edible insects and young adults in a north-east Italian city an exploratory study. British Food Journal 118: 318-326.

Belforti, M., Gai, F., Lussiana, C., Renna, M., Malfatto, V., Rotolo, L., De Marco, M., Dabbou, S., Schiavone, A., Zoccarato, I. and Gasco, L., 2015. *Tenebrio molitor* meal in rainbow trout (Oncorhynchus mykiss) diets: effects on animal performance, nutrient digestibility and chemical composition of fillets. Italian Journal of Animal Science 14: 670-676.

Bishop, C.A., Schulze, M.B., Klaus, S. and Weitkunat, K., 2020. The branched-chain amino acids valine and leucine have differential effects on hepatic lipid metabolism. FASEB Journal 34: 9727-9739.

Bußler, S., Rumpold, B.A., Jander, E., Rawel, H.M. and Schlüter, O.K., 2016. Recovery and techno-functionality of flours and proteins from two edible insect species: meal worm (*Tenebrio molitor*) and black soldier fly (*Hermetia illucens*) larvae. Heliyon 2: e00218.

Chang, M.C. and Tanaka, J., 2002. FT-IR study for hydroxyapatite/collagen nanocomposite cross-linked by glutaraldehyde. Biomaterials 23: 4811-4818.

De Oliveira, F.C., Coimbra, J.S. dos R., De Oliveira, E.B., Zuñiga, A.D.G. and Rojas, E.E.G., 2016. Food protein-polysaccharide conjugates obtained via the maillard reaction: a review. Critical Reviews in Food Science and Nutrition 20: 1108-1125.

Dickinson, E., 2015. Colloids in food: ingredients, structure, and stability. Annual Review of Food Science and Technology 6: 211-233.

Esbensen, K.H. and Swarbrick, B., 2018. Multivariate data analysis: an introduction to multivariate analysis, process analytical technology and quality by design, 6th edition. CAMO Software AS, Montclair, NJ, USA.

Evans, M., Ratcliffe, I. and Williams, P.A., 2013. Emulsion stabilisation using polysaccharide-protein complexes. Current Opinion in Colloid and Interface Science 18: 272-282.

Food and Agriculture Organization and World Health Organization (FAO/WHO), 2013. Dietary protein quality evaluation in human nutrition. Report of an FAO expert consultation. Food and Nutrition Paper no. 92. FAO, Rome, Italy.

Feng, W., Qian, L., Wang, W., Wang, T., Deng, Z., Yang, F., Xiong, J. and Wang, C., 2018. Exploring the potential of lipids from black soldier fly: new paradigm for biodiesel production (II) – extraction kinetics and thermodynamic. Renewable Energy 119: 12-18.

Gu, F., Kim, J.M., Hayat, K., Xia, S., Feng, B. and Zhang, X., 2009. Characteristics and antioxidant activity of ultrafiltrated Maillard reaction products from a casein-glucose model system. Food Chemistry 117: 48-54.

Gu, F.L., Kim, J.M., Abbas, S., Zhang, X.M., Xia, S.Q. and Chen, Z.X., 2010. Structure and antioxidant activity of high molecular weight Maillard reaction products from casein-glucose. Food Chemistry 120: 505-511.

Henderson, J.W., Ricker, R.D., Bidlingmeyer, B.A. and Woodward, C., 2000. Rapid, accurate, sensitive, and reproducible HPLC analysis of amino acids amino acid analysis using Zorbax Eclipse-AAA columns and the Agilent 1100 HPLC. Agilent 20: 1-10.

Henry, M., Gasco, L., Piccolo, G. and Fountoulaki, E., 2015. Review on the use of insects in the diet of farmed fish: past and future. Animal Feed Science and Technology 203: 1-22.

Huang, C., Feng, W., Xiong, J., Wang, T., Wang, W., Wang, C. and Yang, F., 2019. Impact of drying method on the nutritional value of the edible insect protein from black soldier fly (*Hermetia illucens* L.) larvae: amino acid composition, nutritional value evaluation, *in vitro* digestibility, and thermal properties. European Food Research and Technology 245: 11-21.

Ifeduba, E.A. and Akoh, C.C., 2016. Microencapsulation of stearidonic acid soybean oil in Maillard reaction-modified complex coacervates. Food Chemistry 199: 524-532.

Jajić, I., Krstović, S., Glamočić, D., Jakšić, S. and Abramović, B., 2013. Validation of an HPLC method for the determination of amino acids in feed. Journal of the Serbian Chemical Society 78: 839-850.

Janssen, R.H., Vincken, J.P., Van den Broek, L.A.M., Fogliano, V. and Lakemond, C.M.M., 2017. Nitrogen-to-protein conversion factors for three edible insects: *Tenebrio molitor*, *Alphitobius diaperinus*, and *Hermetia illucens*. Journal of Agricultural and Food Chemistry 65: 2275-2278.

Jiménez-Castaño, L., Villamiel, M. and López-Fandiño, R., 2007. Glycosylation of individual whey proteins by Maillard reaction using dextran of different molecular mass. Food Hydrocolloids 21: 433-443.

Kim, T.K., Yong, H.I., Chun, H.H., Lee, M.A., Kim, Y.B. and Choi, Y.S., 2020. Changes of amino acid composition and protein technical functionality of edible insects by extracting steps. Journal of Asia-Pacific Entomology 23: 298-305.

Leiva, G.E., Naranjo, G.B. and Malec, L.S., 2017. A study of different indicators of Maillard reaction with whey proteins and different carbohydrates under adverse storage conditions. Food Chemistry 215: 410-416.

Li, Y., Lu, F., Luo, C., Chen, Z., Mao, J., Shoemaker, C. and Zhong, F., 2009. Functional properties of the Maillard reaction products of rice protein with sugar. Food Chemistry 117: 69-74.

Liu, J., Xu, Q., Zhang, J., Zhao, P. and Ding, Y., 2016. Characterization of silver carp (Hypophthalmichthys molitrix) myosin protein glycated with konjac oligo-glucomannan. Food Hydrocolloids 57: 114-121.

Liu, Q., Kong, B., Han, J., Sun, C. and Li, P., 2014. Structure and antioxidant activity of whey protein isolate conjugated with glucose via the Maillard reaction under dry-heating conditions. Food Structure 1: 145-154.

Lertittikul, W., Benjakul, S. and Tanaka, M., 2007. Characteristics and antioxidative activity of Maillard reaction products from a porcine plasma protein-glucose model system as influenced by pH. Food Chemistry 100: 669-677.

Makkar, H.P.S., Tran, G., Heuzé, V. and Ankers, P., 2014. State-of-the-art on use of insects as animal feed. Animal Feed Science and Technology 197: 1-33.

Mshayisa, V.V. and Van Wyk, J., 2021. *Hermetia illucens* protein conjugated with glucose via Maillard reaction: antioxidant and techno-functional properties. International Journal of Food Science, Article ID: 5572554.

Mshayisa, V.V., 2016. Antioxidant effects of Maillard reaction products (MRPs) derived from glucose-casein model systems. Cape Peninsula University of Technology, Bellville, South Africa.

Müller, A., Wolf, D. and Gutzeit, H.O., 2017. The black soldier fly, *Hermetia illucens* – a promising source for sustainable production of proteins, lipids and bioactive substances. Zeitschrift fur Naturforschung – Section C Journal of Biosciences 72: 351-363.

Muley, A.B., Chaudhari, S.A., Mulchandani, K.H. and Singhal, R.S., 2018. Extraction and characterization of chitosan from prawn shell waste and its conjugation with cutinase for enhanced thermostability. International Journal of Biological Macromolecules 111: 1047-1058.

Niu, L.Y., Jiang, S.T., Pan, L.J. and Zhai, Y.S., 2011. Characteristics and functional properties of wheat germ protein glycated with saccharides through Maillard reaction. International Journal of Food Science and Technology 46: 2197-2203.

Nuthong, P., Benjakul, S. and Prodpran, T., 2009. Characterization of porcine plasma protein-based films as affected by pretreatment and cross-linking agents. International Journal of Biological Macromolecules 44: 143-148.

Osimani, A., Garofalo, C., Milanović, V., Taccari, M., Cardinali, F., Aquilanti, L., Pasquini, M., Mozzon, M., Raffaelli, N., Ruschioni, S., Riolo, P., Isidoro, N. and Clementi, F., 2017. Insight into the proximate composition and microbial diversity of edible insects marketed in the European Union. European Food Research and Technology 243: 1157-1171.

Petrozzi, S., 2013. Practical instrumental analysis: methods, quality assurance and laboratory management. Wiley-VCH Verlag, Weinheim, Germany.

Purschke, B., Meinlschmidt, P., Horn, C., Rieder, O. and Jäger, H., 2018. Improvement of techno-functional properties of edible insect protein from migratory locust by enzymatic hydrolysis. European Food Research and Technology 244: 999-1013.

Phat, C., Moon, B. and Lee, C., 2016. Evaluation of umami taste in mushroom extracts by chemical analysis, sensory evaluation, and an electronic tongue system. Food Chemistry 192: 1068-1077.

Qi, J.R., Yang, X.Q. and Liao, J.S., 2009. Improvement of functional properties of acid-precipitated soy protein by the attachment of dextran through Maillard reaction. International Journal of Food Science and Technology 44: 2296-2302.

Renna, M., Schiavone, A., Gai, F., Dabbou, S., Lussiana, C., Malfatto, V., Prearo, M., Capucchio, M.T., Biasato, I., Biasibetti, E., De Marco, M., Brugiapaglia, A., Zoccarato, I. and Gasco, L., 2017. Evaluation of the suitability of a partially defatted black soldier fly (*Hermetia illucens* L.) larvae meal as ingredient for rainbow trout (Oncorhynchus mykiss Walbaum) diets. Journal of Animal Science and Biotechnology 8: 1-13.

Schiavone, A., De Marco, M., Martínez, S., Dabbou, S., Renna, M., Madrid, J., Hernandez, F., Rotolo, L., Costa, P., Gai, F. and Gasco, L., 2017. Nutritional value of a partially defatted and a highly defatted black soldier fly larvae (*Hermetia illucens* L.) meal for broiler chickens: apparent nutrient digestibility, apparent metabolizable energy and apparent ileal amino acid digestibility. Journal of Animal Science and Biotechnology 8: 51.

Schösler, H., De Boer, J. and Boersema, J.J., 2012. Can we cut out the meat of the dish? Constructing consumer-oriented pathways towards meat substitution. Appetite 58: 39-47.

Su, J.F., Huang, Z., Yuan, X.Y., Wang, X.Y. and Li, M., 2009. Structure and properties of carboxymethyl cellulose/soy protein isolate blend edible films crosslinked by Maillard reactions. Carbohydrate Polymers 79: 145-153.

Sun, Y., Hayakawa, S., Puangmanee, S. and Izumori, K., 2006. Chemical properties and antioxidative activity of glycated α-lactalbumin with a rare sugar, D-allose, by Maillard reaction. Food Chemistry 95: 509-517.

Vhangani, L.N. and Van Wyk, J., 2013. Antioxidant activity of Maillard reaction products (MRPs) derived from fructose-lysine and ribose-lysine model systems. Food Chemistry 137: 92-98.

Wang, C., Qian, L., Wang, W., Wang, T., Deng, Z., Yang, F., Xiong, J. and Feng, W., 2017. Exploring the potential of lipids from black soldier fly: new paradigm for biodiesel production (I). Renewable Energy 111: 749-756.

Waśko, A., Bulak, P., Polak-Berecka, M., Nowak, K., Polakowski, C. and Bieganowski, A., 2016. The first report of the physicochemical structure of chitin isolated from *Hermetia illucens*. International Journal of Biological Macromolecules 92: 316-320.

Young, V.R. and Pellet, P.L., 1991. Protein evaluation, amino acid scoring and the food and drug administration's proposed food labelling regulations. Journal of Nutrition 121: 145-150.

Zhu, D.A.N., Damodaran, S. and Lucey, J.A., 2010. Physicochemical and emulsifying properties of whey protein isolate (WPI)-dextran conjugates produced in aqueous solution. Journal of Agricultural and Food Chemistry 58: 2988-2994.

Zhang, X., Qi, J.R., Li, K.K., Yin, S.W., Wang, J.M., Zhu, J.H. and Yang, X.Q., 2012. Characterization of soy β-conglycinin-dextran conjugate prepared by Maillard reaction in crowded liquid system. Food Research International 49: 648-654.